

The prediction of compressive strength of travertines with special reference to laminae-orientation using index tests

Gholamreza Khanlari *, Fateme Naseri

Department of Geology, University College of Sciences, University of Bu-Ali sina, Hamedan, Iran

*Corresponding author, e-mail: Khanlari_Reza@yahoo.com

(received: 01/02/2017 ; accepted: 19/06/2017)

Abstract

In this research, different experimental techniques have been used to determine the strength of four types of travertines, selected from Hamedan and Markazi Provinces, west and central parts of Iran respectively. For this purpose, after sample preparation and assessment of mineral properties, the selected samples were subjected to physical and mechanical tests with special reference to two major anisotropic angles (i.e. perpendicular (\perp) and parallel (\parallel)) between bedding/lamination planes and the major loading directions. Based on the test results, it can be concluded that the percentage/type of matrix and porosity have a more important effect on the physical and mechanical properties than the rock structure. Statistical analyses, including simple and multiple linear regressions, were applied to identify those physico-mechanical parameters that are more appropriate to predict uniaxial compressive strength ($\sigma_{c\perp}$ and $\sigma_{c\parallel}$) and to establish some new equations. Data analysis in simple regression shows that bulk specific gravity (saturated surface dry, SSD) and Brazilian tensile strength are the most and the least influential factors on $\sigma_{c\perp}$ and $\sigma_{c\parallel}$, respectively. Based on multiple regression method, equations with only two parameters (a physical and a mechanical parameter) were extracted for calculating $\sigma_{c\perp}$ and $\sigma_{c\parallel}$. Among all proposed equations, models 1 and 6 based on SSD-Vp and SSD-CPI variables, seem to be reliable and agreeable to predict $\sigma_{c\perp}$ and $\sigma_{c\parallel}$, respectively. The performance of multiple regression models are evaluated by comparing statistic parameters, including correlation coefficient (R), root mean square error (RMSE), mean error (ME) whose values for $\sigma_{c\perp}$ are 0.86, 11.81, 0.11 and for $\sigma_{c\parallel}$ are 0.86, 12.97, 0.36. Also based on t-test and F-test, all the proposed models in multiple regression, show significant correlations with σ_c at α -level = 0.1.

Keywords: Bedding plane, Petrographical characteristics, Physical properties, Mechanical properties, Multiple regression

Introduction

The uniaxial compressive strength (σ_c) of dimension stones is one of the most important design parameter in rock engineering (Çobanoğlu & Çelik, 2012; Koncagül & Santi, 1999; Mishra & Basu, 2012; Ozcelik *et al.*, 2004). Travertines are widely used across the world in building materials since they are found abundantly and have distinct decorative characteristics. They have had a broad range of use in architectural applications throughout history, including in government buildings, healthcare facilities, hotels, and restaurants (Pentecost, 2005). As shown in Fig. 1a and Fig. 1b, there are some examples of travertine applications in travertine-built heritage buildings in Iran (e.g. Khurheh temple and Atash-koh fire temple). There are several parameters influencing the strength behavior of rocks. These parameters are mineral composition, porosity, fabric (i.e. rock structure and texture), and anisotropy (Saroglou *et al.*, 2004). Many studies have been carried out that aim to investigate the effect of these parameters on strength properties of travertines (Akyol *et al.*, 2005; Chentout *et al.*, 2015; Çobanoğlu and Çelik, 2012; Ersoy *et al.*, 2005; Gokce, 2015; Karakul *et al.*, 2010; Török & Vásárhelyi, 2010). Among these properties, anisotropy plays a significant role on the rock

behavior in engineering projects (Khanlari *et al.*, 2014). Therefore, σ_c of travertine should be assessed regarding rock anisotropy or cutting direction. The strength anisotropy (σ_c) of travertine has been assessed by many researchers in more than two anisotropic angles (Karakul *et al.*, 2010; Ozcelik and Yilmazkaya, 2011; Yilmaz and Yucel, 2014) and other researchers only considered two angles (perpendicular and parallel to the lamination/bedding planes) (Chentout *et al.*, 2015; Çobanoğlu and Çelik, 2012; Garcia-del-Cura *et al.*, 2012; Sengun *et al.*, 2015; Yagiz, 2012).

In recent years, different methods and testing techniques have been developed and implemented to determine strength parameter of anisotropic rocks. Standard procedures for measuring strength parameter of rocks were suggested by (ASTM ; Brown, 1981a). In laboratory testing, strength parameter of intact anisotropic rocks is usually determined from specimens prepared at different angles with respect to the apparent planes of anisotropy. The most important laboratory static tests include uniaxial and triaxial compression tests. Literature review shows that performing direct static laboratory tests in order to evaluate rock strength and deformation is mostly expensive and requires considerable time due to preparation of rock

specimens. Therefore, different indirect testing methods were developed and used to interpret the strength parameter of anisotropic rocks. These tests are relatively easy to perform, cheap, and take short testing time (Shalabi *et al.*, 2007). These indirect index tests have been applied to develop different predictive models such as regression analyses, fuzzy inference system and neural network approaches for measuring σ_c (Cargill & Shakoor, 1990; D'Andrea *et al.*, 1965; Dehghan *et al.*, 2010; Karakul *et al.*, 2010; Kohno & Maeda, 2012; Shakoor and Bonelli, 1991; Sharma & Singh, 2008; Singh *et al.*, 2001; Sulukcu and Ulusay, 2001; Torabi-Kaveh *et al.*, 2015; Ulusay *et al.*, 1994; Vernik *et al.*, 1993; Yagiz, 2009; Yesiloglu-Gultekin *et al.*, 2013). Among these techniques, simple and multiple regression techniques are more commonly used to establish a predictive model (Gokceoglu, 2002). Despite the wide use of these index tests for determining strength property of anisotropic rocks, a few studies have been done to determine σ_c of anisotropic rocks especially travertines using the multiple regression technique.

Accordingly, the present study aimed: i) to investigate the effects of mineralogical content, fabric, porosity and anisotropy angle (cutting direction) on strength of travertine, simultaneously; ii) to evaluate the potential of different index tests such as Brazilian strength test (σ_t), axial and diametral point load test ($I_{s(a)}$ and $I_{s(d)}$), cylindrical punch index test (CPI), block punch index test (BPI), and physical properties (effective porosity (n_ϕ), dry density (γ_d), quick water absorption (QAI) and saturated surface dry density (SSD)) for measuring strength anisotropy of travertine with different structures; and iii) to present some statistical models for predicting strength anisotropy of rocks using one physical and one mechanical parameters.

Materials and methods

In this study, four types of travertines including cream (CDH) and walnut (WDH), snake skin (SKM) and white (WAM) travertines, were selected for investigation. These rocks crop out in Hamedan and Markazi Provinces, respectively (Fig. 2). As shown in figure (3), cream (CDH) and walnut (WDH) travertines were selected from Hamedan province (Dingle-kahriz village) and snake skin (SKM) and white (WAM) travertines from Markazi province (Khurheh and Atash-koh villages). It is noteworthy that the SKM travertines have been applied in different construction elements of Khurheh temple, especially the columns cut from blocks that are

parallel to the bedding/lamination planes (Fig. 1a). WAM travertines were, also, utilized as rubble stones in the construction of Atash-koh fire temple located in Mahalat city, Markazi Province (Fig. 1b).

Laboratory studies

Samples were obtained from active quarries especially fresh and unweathered outcrops. For each type of travertine, about 10 blocks of each rock type ($50 \times 80 \times 80$ cm) were prepared, each of which was capable of providing 40 core samples with the length of 35 to 40 cm. The blocks were transferred to the geotechnical laboratory of Bu-Ali Sina university where the cylindrical cores were extracted using a core drilling machine. Then, cut end faces of the obtained cores were smoothed very accurately perpendicular to the axis of a cylindrical part using a lathe machine.

A total of 1440 specimens (4 rock types \times 10 blocks for each rock type \times 3 specimens extracted from each block \times 6 mechanical tests \times 2 cutting directions) were prepared for Brazilian tensile test, uniaxial compressive test, cylindrical punch test, block punch test, and diametral and axial point load tests at parallel and perpendicular to the lamination/bedding axes. As mentioned earlier, 10 blocks were prepared for each rock type and 3 specimens were extracted from each block. Therefore, a total of 30 specimens for each aforementioned test were used. Specimen thickness of block and cylindrical punch tests (BPI and CPI tests) were kept between 5 and 15 mm as prescribed by Ulusay *et al.*, (2001). Length to diameter ratio (L/D) of the diametral ($L/D > 1$) and axial ($L/D = 0.3 - 1$) point load test ($I_{s(d)}$ and $I_{s(a)}$) specimens were in accordance with the ISRM (1985) specification (Franklin, 1985).

Brazilian tensile (σ_t) and uniaxial compressive tests (σ_c) were performed according to ISRM, (1978) and ISRM, (1979) stipulations with L/D ratios of 0.5-0.75 and 2-2.5, respectively (Brown, 1981b; ISRM, 1978). The core diameter for these tests covered the NX (54 mm) core sizes, commonly used in geotechnical investigations. A general view of all test apparatus used in this study is given in Fig. 4. Finally, physical properties including: dry density (γ_d), quick water absorption index (QAI) (Ersoy *et al.*, 2005), effective porosity (n_ϕ) (Rilem, 1980), and bulk specific gravity (saturated surface dry-SSD) (ASTM, 2005) were measured on the same specimens subjected to uniaxial compressive strength test.

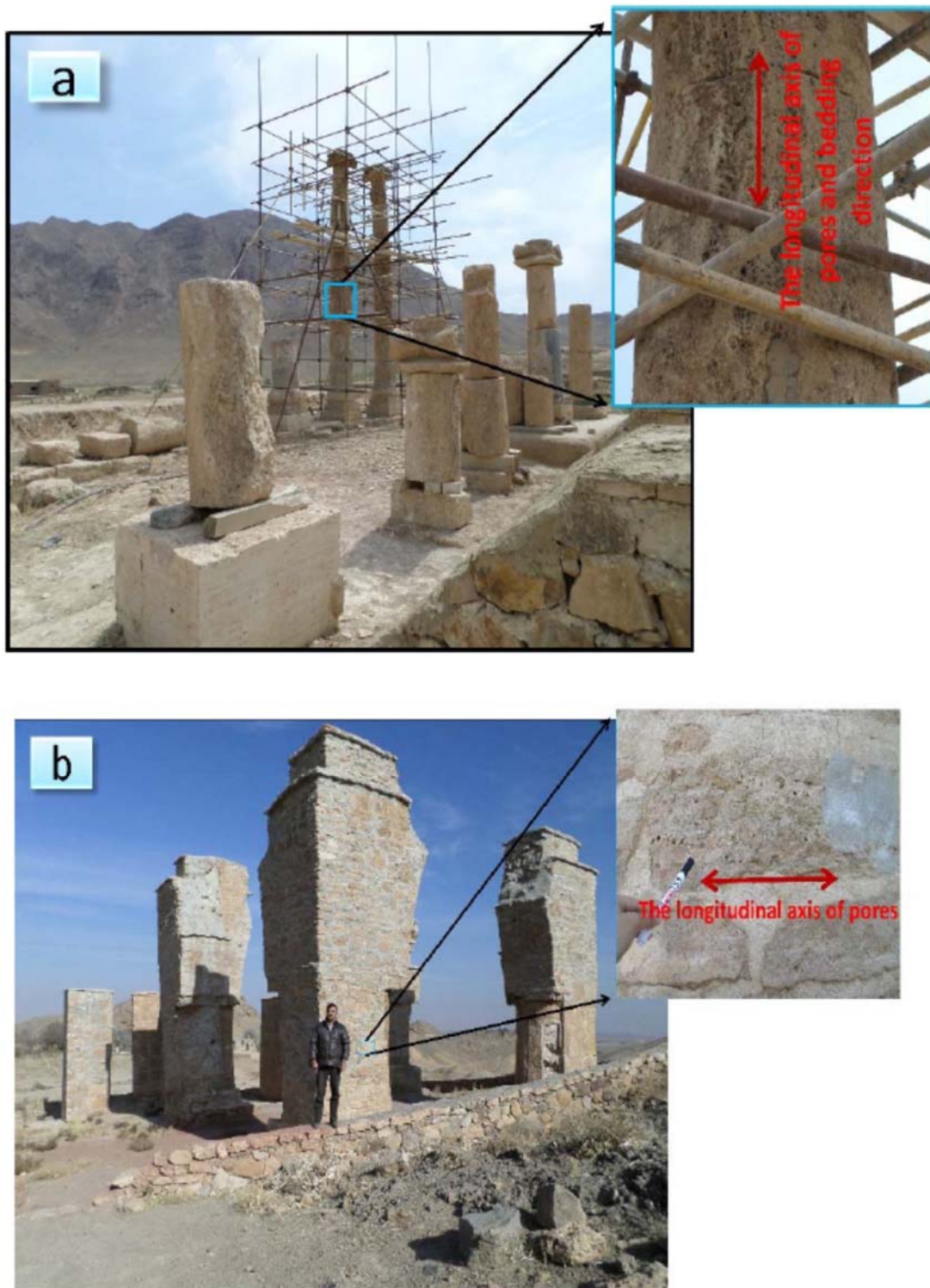


Figure 1. Mahallat's travertine ancient monuments. a: Khurheh temple (Parthian age), b: Atash-koh fire temple (Sassanid age) (The red arrows show the bedding plane direction and the longest axis of pores)

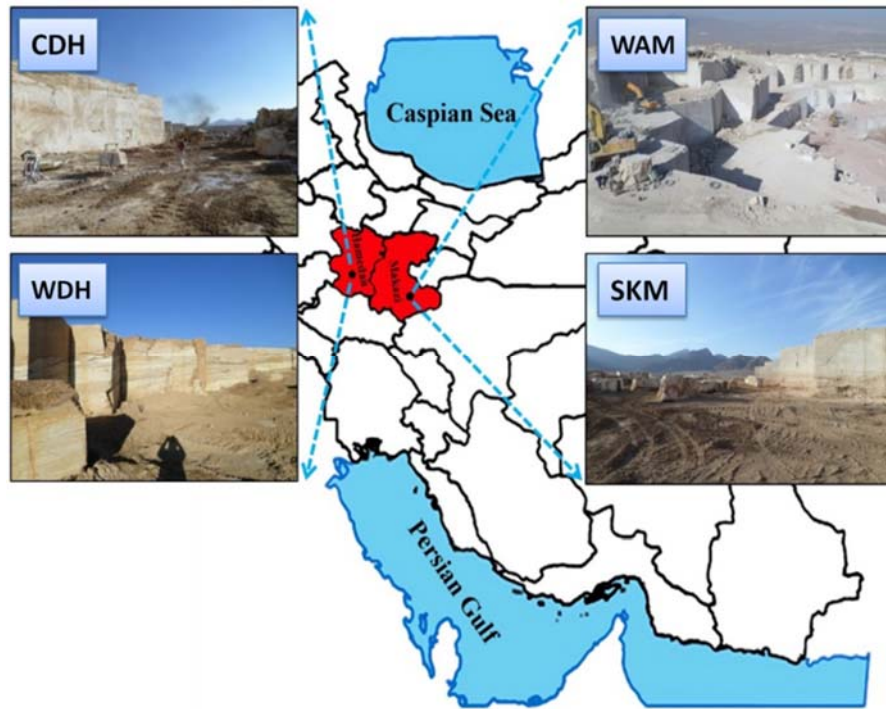


Figure 2. Travertine quarries and sampling locations under study (Hamedan province: CDH and WDH samples); Markazi province: WAM and SKM samples)

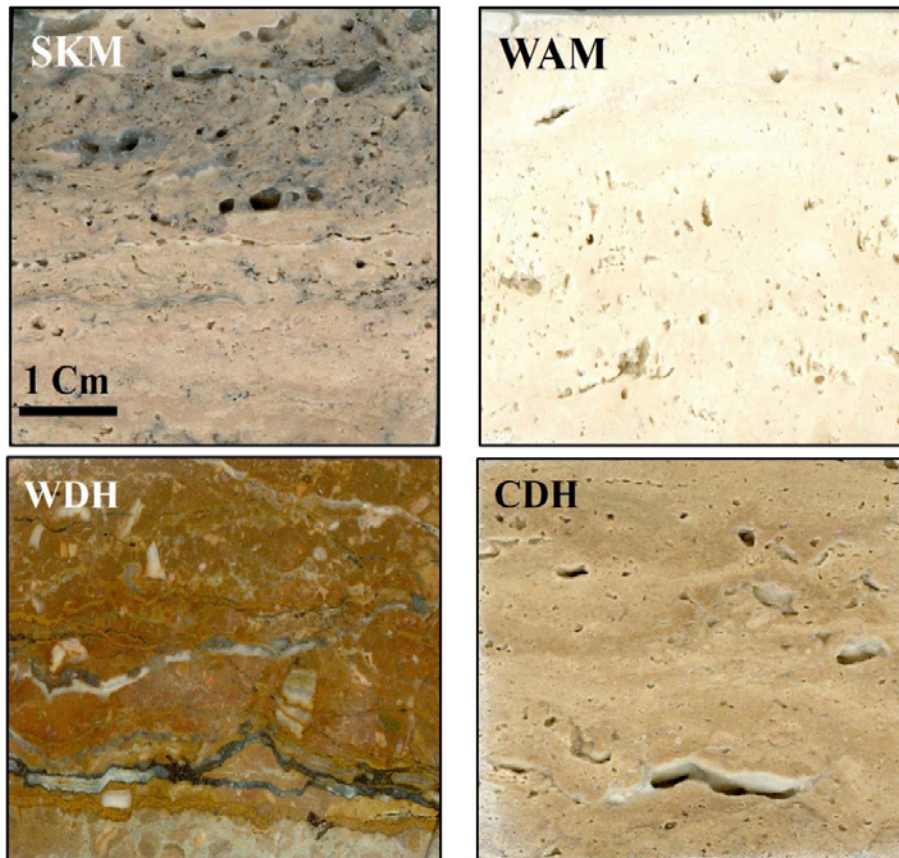


Figure 3. Tested rocks and lamination/bedding planes.

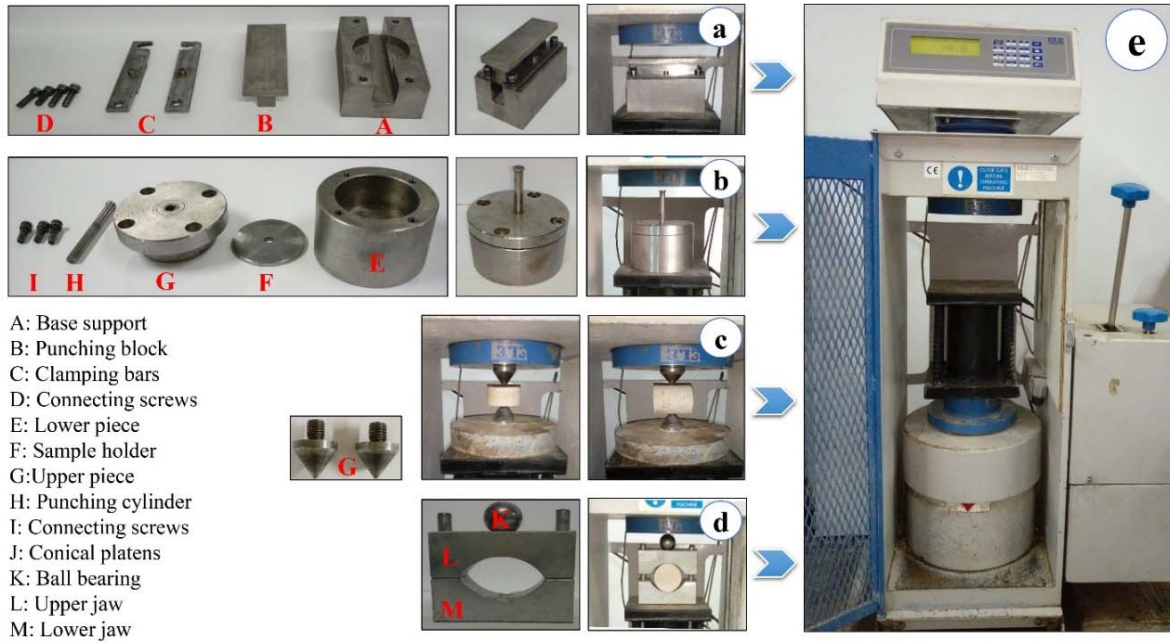


Figure 4. A general view of all test apparatus used in this study; (a) Block punch, (b) Cylindrical punch, (c) Point load, (d) Brazilian tensile, and (e) Uniaxial compressive test setups.

Statistical analyses

In this section, regression modeling technique was used to evaluate the relationship between σ_c and other geomechanical parameters. In this study, the multiple linear regression model was applied using Minitab 14 statistical software. A general linear regression model with k repressor in matrix form can be expressed as

$$Y_{n \times 1} = X_{n \times p} B_{p \times 1} + \epsilon_{n \times 1} \quad (1)$$

where Y is an $n \times 1$ vector of vector of observations (i.e. dependent variable or responses), B is a $p \times 1$ vector of parameters (i.e. regression coefficients), X is a $n \times p$ matrix of constants involving the levels of the regression variables (explanatory or independent variables), ϵ is a $n \times 1$ vector of normal random errors, and $p=k+1$ (Montgomery *et al.*, 2015).

For the current study, the uniaxial compressive strength (parallel and perpendicular to the bedding/lamination axis; $\sigma_{c\perp}$ and $\sigma_{c\parallel}$) was correlated statistically with the 10 intact rock properties. In addition, correlation coefficient (R), root mean square error (RMSE), mean error (ME), t-test and F-test were used as standard statistical metrics to check the validity and quality of the regression model obtained. The formulas are Eqs. 2-4:

$$R = \frac{N(\sum y_i \hat{y}_i) - (\sum y_i)(\sum \hat{y}_i)}{\sqrt{[N\sum y_i^2 - (\sum y_i)^2]} \sqrt{N\sum \hat{y}_i^2 - (\sum \hat{y}_i)^2}} \quad (2)$$

$$RMSE = \sqrt{\frac{\sum_{i=1}^N (y_i - \hat{y}_i)^2}{N}} \quad (3)$$

$$ME = \frac{\sum_{i=1}^N (y_i - \hat{y}_i)}{N} \quad (4)$$

where, N is the total number of measured data points; y_i is the measured σ_c ; \hat{y}_i is the predicted σ_c .

The correlation coefficient (R) (Eq. 2) is used as a relative measure of model fitness. The model with R value close to -1 or +1 can be considered as the best one. In other words, its absolute value indicates the strength, and so the larger value of R expresses stronger relationship (Ghorbani Dashtaki *et al.*, 2009). Equation (3) is used to calculate the mean prediction error for each model and for an ideal one it should be close to zero. The optimal network that gives the lowest RMSE is selected as an optimal model (Suwansawat and Einstein, 2006). The ME (Eq. 4) is tested to show the worst state of a predicted model. It is close to zero for a good estimation. The difference between RMSE and ME value is a good indicator for the presence and extent of outliers, or variance of the differences between the modeled and observed values (Legates and McCabe, 1999). In addition, the ME statistic indicates whether the selected model overestimates or underestimates the measurements (Ghorbani Dashtaki *et al.*, 2009).

Beside these statistics, student's t-test has been used in this study to demonstrate validity and reliability of models/equations by significant. As this test was performed at 90 % significance level, the significance (P-value) should be less than 0.1. The t statistic can be calculated as follows (Eq. 5):

$$t = \frac{\bar{X} - \bar{Y}}{S_p \sqrt{\frac{1}{n} + \frac{1}{m}}}, \quad S_p^2 = \frac{(n-1)S_x^2 + (m-1)S_y^2}{n+m-2} \quad (5)$$

where, \bar{X} and \bar{Y} are the sample means, S_p^2 is the pooled variance of the two samples, S_x and S_y are the sample standard deviations of X and Y, and n and m are the sample sizes. The denominator of t is the standard error of the difference between two means. The t value is positive if the first mean is larger than the second and negative if it is lower. Once the t value is computed, it is then compared with the tabulated value. If the computed value is larger than the tabulated one, then it indicates strong and significant correlation. The tabulated t is 1.64 at 90 % significance level and all computed t should be higher than this value, which means the significance (P-value) is less than 0.1 (Khanlari *et al.*, 2012; Sharma *et al.*, 2011). The F-test is hypothesis test that examines the variances of two groups to determine their equality and the validity of the overall model. F-test is conducted as follows (Eq. 6):

$$F = \frac{S_1^2}{S_2^2} \quad (6)$$

where, S_1^2 = variance of the first sample and S_2^2 =

variance of second sample. The degree of freedom for the numerator is n_1-1 and for the denominator is n_2-1 . Typically, one-tailed F-test refers to the F-distribution. If the computed F-value is greater than a critical value from the F-distribution, then at least one of the coefficients is not equal to zero. Also, the critical value of F statistic is 1.50 at 90 % significance level and the computed F should be higher than this value which means the significance (P-value) is less than 0.1 (Montgomery *et al.*, 2015).

Results and discussion

Mineralogical descriptions

Due to different depositional conditions, travertines can be distinguished from each other in terms of their color, appearance, porosity, texture, and structure (Erdoğan and Özvan, 2015).

Mineralogical and petrographic features in block samples were examined using an optical microscope. Then, the mineralogical abundance of the specimens was recorded and their textural, structural and microstructural features were characterized. Thin sections were prepared in two cutting directions (parallel and perpendicular) to the bedding/lamination axis. Five thin-sections for each direction and a total of 10 thin sections were prepared for each type of travertine.

A summary of the petrographical properties of different tested travertines is given in Table 1. The travertines were classified according to their relative proportions of allochems to matrix, type of matrix, carbonate content, and fabric characteristics (Zarif & Tuğrul, 2003). The samples were classified according to Folk's (1962) classification scheme.

Table 1 Mineralogical and petrographical features (Para: parallel; Perp: perpendicular; W-Para: white band-parallel; B-Para: Black band-parallel)

Rock code	Thin section direction to the lamination	Folk's classification (1969)	Matrix		Structure	Texture	Porosity (%)
			Sparite (%)	Micrite (%)			
CDH	Para	Pelmicrite	20	80	Massive (>10 cm)	Peloidal texture	5.4
	Perp	Pelmicrite	20	80	Cryptolaminated	laminated texture	10.58
SKM	W- Para	Pelmicrite	20	80	Massive (>10 cm)	Peloidal texture	1.72
	B- Para	Biosprite	40	60	Massive (>10 cm)	Clotted texture	5.2
	Perp	Biomicrite	35	65	Banded (>1 cm)	Laminated texture	7.2
WAM	Para	Biopelmicrite	15	85	Massive (>10 cm)	Peloidal texture	3.2
	Perp	Biopelmicrite	15	85	Massive (>10 cm)	Algal laminated texture, Peloidal texture	6.05
WDH	Para	Intrapelmicrite	30	70	Massive (>10 cm)	Clotted texture	1.33
	Perp	Biolithite	50	50	Laminated (<1 cm)	Laminated texture	4.4

As shown in Figs. 5 and 6, the studied rocks are mainly composed of calcite predominated by two types of matrixes including microcrystalline carbonate mud (micrite) and the coarse crystalline calcite cement (sparite). In addition, peloid, algal materials and intraclasts provide the main allochems of the studied travertines (Table 1). It is notable that the WDH and WAM samples have the most and the least sparite cement content respectively. Moreover,

SKM sample shows higher values of sparite cement content than CDH sample.

According to this classification, the studied rocks are divided into six types of travertine: 1) pelmicrite (CDH and SKM-para), 2) biosparite (SKM-para), 3) biopelmicrite (WAM), 4) biomicrite (SKM-perp), 5) biolithite (WDH-perp), and 6) Intrapelmicrite (WDH-para).

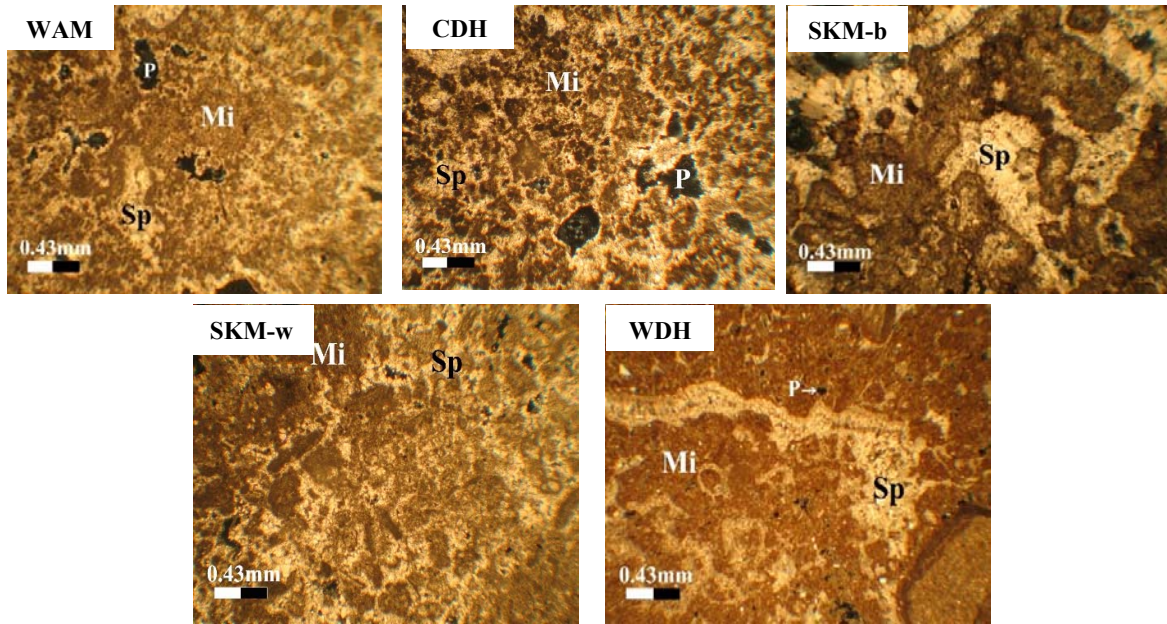


Figure 5. Photomicrogrphs of the studied travertines (The images are parallel (para) to the lamination/bedding axes, Sp: Sparite; Mic: Micrite; P: porosity)

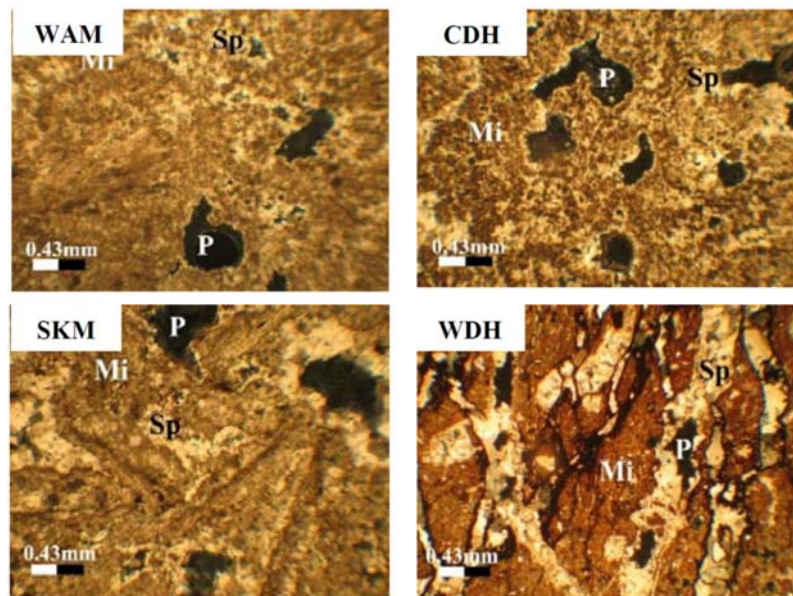


Figure 6. Photomicrogrphs of the studied travertines (The images are perpendicular (perp) to the lamination/bedding axis, Sp: Sparite; Mic: Micrite; P: porosity)

Considering the analyses of thin-sections, based on the geometric characteristic of the bedding/lamination four different structures were found in the studied travertines: massive (average layer thickness greater than 10 cm), banded (layers between 1 and 10 cm), laminated (commonly 0.05 to 1 cm thick) and cryptolaminated (millimeter layers only clearly visible under optical microscopy) structures. It is worth mentioning that all travertine types have massive structure in thin sections with the parallel direction to the lamination/bedding axis. Although, a microscopic massive structure appeared for all specimens, the orientation of pores led to create the anisotropic appearance on the macroscopic scale.

From the thin sections, it can easily be seen that three different textures including peloidal, clotted and laminated are dominant in the studied rocks. From thin sections, the average porosity was determined and reported in Table 1. In all tested samples, a higher porosity percentage was achieved through perpendicular loading conditions to the lamination/bedding axis than parallel loading conditions. Besides, the porosity percentage in the studied travertines for both cutting directions is in the order of $WDH < WAM < SKM < CDH$.

Physical properties

Physical properties of different intact rocks are generally determined by their mineral compositions and microstructures (Khanlari *et al.*, 2014). These properties are strongly influenced by the texture, structure and the minerals forming the rocks (Irfan, 1996). Tables 2 and 3 show the values of the physical parameters for the tested samples.

As mentioned earlier, the studied travertines present four kinds of structures termed as massive (WAM), banded (SKM), laminated (WDH) and cryptolaminated (CDH). The rocks with cryptolaminated structure can be porous or have low porosity ($n_\phi = 3.96-9.26\%$), whereas those with massive, banded and laminated structures only are less porous ($n_\phi < 6\%$).

As seen in Tables 2 and 3, the travertines with laminated structure show a very low and limited range of porosity ($n_\phi = 2.11-3.96\%$), while travertines with cryptolaminated structure indicate a reverse behavior with wide range of porosity ($n_\phi = 3.96-9.26\%$). Consequently, the amount of porosity couldn't be a suitable factor for distinguishing the type of structure in travertines. However, Török and Vásárhelyi, (2010) reported a complete opposite conclusion. Their results revealed that the structure

of the travertine can be predicted from their effective porosity, because the blocks having porosity lower than 5% usually belong to the massive structure and blocks with porosity higher than 5% belong to the laminated structure.

The average values of the SSD and γ_d of the studied samples for both cutting directions is in the order: $WDH > WAM > SKM > CDH$. Thus, the laminated and the cryptolaminated structures have the most and the least SSD and γ_d values respectively. Furthermore, other physical parameters (n_ϕ and QAI) show a reverse order for all kinds of travertines at perpendicular cutting direction ($WDH < WAM < SKM < CDH$).

The V_p values were found to have an increasing trend ($CDH < SKM < WAM < WDH$) with a decrease in n_ϕ for travertines parallel to the loading direction. Thus, it can be stated that the banded, laminated and massive structures have a less considerable effect on the V_p parameter. This ascending trend in V_p values from high porous (CDH) to low porous (WDH) specimens was not observed in samples perpendicular to loading conditions. WDH samples, which have the lowest porosity, presented lower V_p values in comparison to WAM and SKM samples, concerning the fact that this rock has laminations and higher sparite content ($SP = 50\%$). Therefore, the increase in sparite content (crystal size) cause a decrease in V_p values.

According to the obtained results, V_p values for perpendicular to the lamination/bedding planes showed lower values than parallel direction to lamination/bedding axis. This behavior is to be expected, as the propagation of ultrasonic waves is easier in samples with parallel direction to the lamination/bedding. The results are consistent with the data published in the bibliography (García-del-Cura *et al.*, 2012; Saroglou *et al.*, 2004).

Mechanical properties

The results of mechanical tests, performed on the travertine samples for both directions, parallel and perpendicular to the lamination/bedding axis, are reported in Tables 2 and 3. The mechanical tests conducted in the present study are Brazilian tensile strength, uniaxial compressive strength, cylindrical punch, block punch and diametral/axial point load tests.

All these tests yield strength indices in a simple and practical way, employing which it is possible to indirectly determine uniaxial compressive strength (σ_c). As mentioned before, a total of 30 samples were used for each mechanical test.

Table 2. Results of physico-mechanical parameters at parallel to the lamination/bedding axis

Rock code	Block no.	γ_d	$n\phi$	SSD	QAI	σ_t	$I_s(a)$	$I_s(d)$	Vp	CPI	BPI	σ_c
		(g/cm ³)	(%)	-	(%)	(MPa)	(MPa)	(MPa)	(km/s)	(MPa)	(MPa)	(MPa)
CDH	1	2.39	5.08	2.46	2.00	5.70	2.69	3.04	5.01	2.94	10.65	62.94
CDH	2	2.42	5.90	2.47	2.34	4.37	2.95	2.20	4.07	1.66	13.75	59.49
CDH	3	2.41	6.23	2.47	2.47	7.89	3.14	2.70	4.90	2.20	10.85	48.70
CDH	4	2.42	7.00	2.47	2.79	4.46	2.80	2.37	5.05	2.13	11.76	45.35
CDH	5	2.36	7.16	2.42	2.86	7.34	2.43	1.69	3.78	1.49	10.43	39.77
CDH	6	2.35	7.42	2.42	2.98	6.31	2.66	2.53	4.08	1.84	9.99	45.40
CDH	7	2.38	7.77	2.43	3.14	6.22	2.95	2.37	4.15	1.24	9.08	36.77
CDH	8	2.35	8.36	2.42	3.39	6.58	3.01	2.03	4.05	2.59	9.63	47.14
CDH	9	2.39	8.46	2.45	3.45	6.49	2.44	2.36	4.08	1.49	8.82	44.09
CDH	10	2.39	8.35	2.46	3.37	7.76	3.28	2.37	4.10	1.03	7.48	58.54
	Ave	2.39	7.17	2.45	2.88	6.31	2.84	2.37	4.33	1.86	10.24	48.82
	Sd Dev	0.03	1.14	0.02	0.49	1.22	0.28	0.36	0.47	0.6	1.72	8.72
SKM	1	2.45	3.75	2.51	1.52	4.99	3.21	3.05	5.03	1.91	12.15	57.77
SKM	2	2.45	3.79	2.50	1.54	6.14	2.88	4.07	5.16	1.57	13.90	69.40
SKM	3	2.42	4.26	2.49	1.74	4.55	4.26	3.05	4.81	2.80	8.97	54.83
SKM	4	2.10	4.10	2.47	1.69	5.74	2.54	2.54	4.96	2.19	10.83	53.90
SKM	5	2.37	4.59	2.45	1.91	5.56	2.25	2.54	4.77	1.50	6.12	46.20
SKM	6	2.46	3.50	2.51	1.41	6.74	3.60	3.74	5.09	2.04	11.73	71.36
SKM	7	2.37	5.02	2.45	2.09	7.50	2.72	3.23	4.96	1.49	8.20	58.46
SKM	8	2.40	3.98	2.47	1.64	6.58	3.89	2.71	5.04	2.94	7.48	71.73
SKM	9	2.43	3.16	2.49	1.29	6.47	3.83	3.39	4.91	2.89	10.94	63.09
SKM	10	2.41	4.50	2.48	1.85	4.84	3.16	2.88	4.85	2.99	7.90	37.87
	Ave	2.39	4.07	2.48	1.67	5.91	3.23	3.12	4.96	2.23	9.82	58.46
	Sd Dev	0.10	0.55	0.02	0.24	0.94	0.65	0.5	0.12	0.62	2.45	11.02
WAM	1	2.45	3.08	2.50	1.25	8.10	4.88	3.41	4.67	2.44	17.48	75.38
WAM	2	2.43	3.80	2.49	1.55	8.14	3.99	4.18	4.68	4.71	11.63	98.20
WAM	3	2.38	4.50	2.46	1.87	7.19	4.36	2.38	4.79	2.35	8.28	40.87
WAM	4	2.45	3.43	2.51	1.39	9.31	3.32	2.90	4.63	3.21	16.61	73.73
WAM	5	2.39	5.08	2.46	2.00	7.72	4.06	3.75	4.84	3.96	11.90	58.91
WAM	6	2.38	4.97	2.46	2.06	7.62	2.77	2.45	4.65	2.48	9.72	68.49
WAM	7	2.41	3.63	2.48	1.49	8.14	3.63	3.90	4.86	3.56	14.86	55.28
WAM	8	2.42	4.72	2.48	1.95	7.62	3.78	3.25	4.64	1.89	7.76	71.10
WAM	9	2.41	4.20	2.48	1.72	6.12	2.90	3.41	4.99	3.62	15.23	82.69
WAM	10	2.37	4.70	2.43	1.97	6.22	4.15	2.90	4.63	2.29	8.00	35.48
	Ave	2.41	4.21	2.47	1.72	7.62	3.78	3.25	4.74	3.05	12.15	66.01
	Sd Dev	0.03	0.69	0.02	0.29	0.94	0.65	0.60	0.12	0.9	3.69	18.93
WDH	1	2.53	2.28	2.61	0.93	8.90	6.76	4.75	5.75	2.99	16.22	113.53
WDH	2	2.47	2.50	2.58	1.03	9.27	4.97	3.88	5.30	3.74	9.58	97.74

WDH	3	2.46	3.01	2.55	1.25	6.27	4.98	3.90	5.41	2.54	12.74	52.59
WDH	4	2.52	2.36	2.59	0.97	6.10	3.94	4.24	5.40	2.44	17.21	85.55
WDH	5	2.48	2.71	2.56	1.13	8.51	4.27	3.04	5.24	2.80	11.62	68.73
WDH	6	2.44	3.27	2.54	1.35	6.50	3.62	3.71	4.85	2.02	9.23	49.18
WDH	7	2.51	2.38	2.58	0.97	9.69	5.50	4.08	5.33	4.62	17.61	116.20
WDH	8	2.45	3.12	2.56	1.29	5.24	3.34	3.90	4.81	3.12	7.74	74.45
WDH	9	2.49	2.65	2.58	1.11	5.55	4.15	4.08	5.32	2.97	11.99	103.46
WDH	10	2.46	3.06	2.55	1.28	5.71	4.54	3.40	5.09	4.42	12.57	89.92
	Ave	2.48	2.73	2.57	1.13	7.17	4.61	3.90	5.25	3.17	12.65	85.13
	Sd Dev	0.03	0.36	0.02	0.15	1.71	1.0	0.46	0.28	0.85	3.41	23.63

γ_d : dry density, n_ϕ : effective porosity, SSD: bulk specific gravity, QAI: quick water absorption, σ_t : Brazilian tensile strength, $I_{s(a)}$: axial point load, $I_{s(d)}$: diametral point load, Vp: ultrasonic wave velocity, CPI: cylindrical punch index, BPI: block punch index, and σ_c : uniaxial compressive strength.

Table 3 Results of physico-mechanical parameters at perpendicular to the lamination/bedding axis

Rock code	Block no.	γ_d	n_ϕ	SSD	QAI	σ_t	$I_{s(a)}$	$I_{s(d)}$	Vp	CPI	BPI	σ_c
		(g/cm ³)	(%)	-	(%)	(MPa)	(MPa)	(MPa)	(km/s)	(MPa)	(MPa)	(MPa)
CDH	1	2.34	6.83	2.43	2.72	6.06	4.02	2.53	3.84	2.52	4.73	50.44
CDH	2	2.37	8.44	2.44	3.40	6.93	4.06	2.19	4.16	1.01	4.32	49.34
CDH	3	2.36	4.79	2.46	1.88	5.95	3.71	2.72	4.11	2.51	4.40	28.47
CDH	4	2.32	7.18	2.41	2.87	6.52	4.08	2.37	3.75	1.43	7.55	52.96
CDH	5	2.36	5.62	2.44	2.21	6.38	3.25	3.88	3.77	1.16	4.27	34.13
CDH	6	2.34	9.26	2.43	3.75	5.79	2.27	2.37	4.72	1.71	7.27	20.13
CDH	7	2.48	5.34	2.47	2.09	8.16	4.40	2.37	3.77	1.45	5.32	57.03
CDH	8	2.38	7.89	2.46	3.15	6.29	3.80	2.53	4.79	1.78	7.49	46.68
CDH	9	2.35	6.24	2.45	2.48	8.68	2.86	2.36	4.63	1.32	6.13	47.79
CDH	10	2.39	3.96	2.47	1.54	5.97	3.92	2.10	4.55	2.00	7.60	38.23
	Ave	2.37	6.55	2.45	2.61	6.67	3.64	2.54	4.21	1.69	5.91	42.52
	Sd Dev	0.04	1.68	0.02	0.70	0.99	0.65	0.50	0.42	0.52	1.46	11.84
SKM	1	2.46	2.84	2.47	1.16	5.90	4.31	3.06	4.86	3.16	8.19	42.63
SKM	2	2.39	3.96	2.47	1.54	5.33	3.97	3.21	4.56	1.42	7.62	53.48
SKM	3	2.51	4.24	2.47	1.75	6.65	4.87	3.39	4.48	2.63	6.96	43.56
SKM	4	2.31	6.05	2.45	2.53	3.33	3.10	3.16	4.67	1.75	6.86	45.05
SKM	5	2.38	4.70	2.47	1.94	6.02	4.49	3.73	4.62	2.61	7.60	50.31
SKM	6	2.39	4.10	2.47	1.69	7.96	4.62	3.22	4.91	2.14	6.73	52.97
SKM	7	2.41	3.47	2.49	1.41	5.83	4.06	2.89	4.95	1.85	8.19	45.58
SKM	8	2.44	3.69	2.52	1.49	6.00	4.57	3.39	4.65	1.82	7.93	53.38
SKM	9	2.33	5.13	2.43	2.16	4.62	3.74	2.71	4.52	3.05	7.30	35.51
SKM	10	2.51	5.66	2.44	2.37	6.43	3.83	2.88	4.49	2.30	9.77	28.06
	Ave	2.41	4.38	2.47	1.81	5.81	4.16	3.16	4.67	2.27	7.71	45.05
	Sd Dev	0.07	1.00	0.02	0.44	1.23	0.53	0.30	0.18	0.58	0.89	8.29
WAM	1	2.44	4.15	2.51	1.68	6.08	4.94	2.38	4.73	6.24	14.65	56.40
WAM	2	2.39	4.89	2.47	2.02	6.60	5.17	2.89	4.65	3.31	11.44	61.39
WAM	3	2.45	3.42	2.51	1.38	10.08	5.43	3.13	4.63	3.92	12.11	44.90
WAM	4	2.39	3.96	2.47	1.54	7.32	4.49	2.38	4.69	2.14	13.07	49.41
WAM	5	2.45	3.91	2.52	1.58	7.89	5.15	2.76	4.61	3.24	10.28	49.30

WAM	6	2.43	5.32	2.51	2.16	8.36	3.59	2.93	4.69	3.32	13.12	51.93
WAM	7	2.45	3.74	2.51	1.52	5.50	4.64	2.55	4.72	2.13	10.74	39.91
WAM	8	2.45	4.48	2.51	1.82	9.49	3.99	3.49	4.52	3.75	11.53	60.32
WAM	9	2.46	4.07	2.52	1.65	7.70	5.51	3.68	4.79	1.45	7.77	46.68
WAM	10	2.49	3.19	2.53	1.28	6.24	5.49	3.58	4.90	2.88	11.16	59.11
	Ave	2.44	4.11	2.50	1.66	7.53	4.84	2.98	4.69	3.24	11.59	51.93
	Sd Dev	0.03	0.64	0.02	0.27	1.49	0.66	0.48	0.10	1.31	1.87	7.20
WDH	1	2.50	3.04	2.58	1.27	5.82	6.95	3.68	4.50	3.09	14.10	80.05
WDH	2	2.47	3.57	2.57	1.48	7.59	6.39	3.78	4.19	4.92	12.59	85.81
WDH	3	2.53	2.49	2.61	1.02	7.80	5.47	3.73	4.48	3.22	12.50	40.31
WDH	4	2.49	3.22	2.58	1.35	8.74	4.86	4.47	4.37	4.57	11.25	72.78
WDH	5	2.53	2.78	2.61	1.16	8.67	5.10	4.05	4.31	3.06	15.56	66.75
WDH	6	2.45	3.96	2.56	1.66	7.08	5.59	4.30	4.05	2.29	10.78	70.05
WDH	7	2.52	2.60	2.61	1.07	7.02	4.24	4.33	4.28	4.36	14.75	96.27
WDH	8	2.50	3.42	2.58	1.41	6.51	4.76	4.09	4.46	2.81	17.94	78.03
WDH	9	2.52	2.90	2.58	1.20	8.62	5.63	4.45	4.21	4.58	10.29	74.45
WDH	10	2.57	2.11	2.62	0.86	9.21	5.41	3.88	4.15	4.62	10.92	86.50
	Ave	2.51	3.01	2.59	1.25	7.71	5.44	4.08	4.30	3.75	13.07	75.10
	Sd Dev	0.03	0.55	0.02	0.24	1.10	0.79	0.30	0.15	0.95	2.48	15.05

γ_d : dry density, $n\phi$: effective porosity, SSD: bulk specific gravity, QAL: quick water absorption, σ_t : Brazilian tensile strength, I_s (a): axial point load, I_s (d): diametral point load, Vp: ultrasonic wave velocity, CPI: cylindrical punch index, BPI: block punch index, and σ_c : uniaxial compressive strength.

Brazilian tensile strength

The Brazilian tensile strength values of CDH, SKM, WAM and WDH specimens are 6.31, 5.91, 7.62 and 7.17 for parallel to the lamination/bedding axis, while the values for perpendicular direction are 6.67, 5.81, 7.53 and 7.71, respectively. As WDH and CDH have respectively the minimum and maximum $n\phi$ values, it was expected to also have the maximum and minimum σ_t values. However, it was found that WAM and SKM show the maximum and minimum σ_t values for cut parallel to the lamination/bedding planes. This behavior might be explained by the existence of black porous bands in SKM and disorder laminations in WDH samples that led to decrease in σ_t values in comparison to the CDH and WAM specimens. The black porous bands of SKM that are between 2 or 3 cm wide sometimes affect the results of σ_t test. The σ_t values in both cutting directions show that nearly all types of travertines have lower σ_t values for direction perpendicular to the lamination/bedding.

Point load strength

As previously discussed, the point load test was axially ($I_{s(a)}$) and diametrically ($I_{s(d)}$) performed on dried cylindrical specimens in perpendicular and parallel to the lamination/bedding axis. As Tables 2 and 3 show $I_{s(a)}$ and $I_{s(d)}$ values in both cutting

directions are in the order of $CDH < SKM < WAM < WDH$. In addition, $I_{s(a)}$ and $I_{s(d)}$ values at perpendicular direction are higher than those in a parallel direction in all travertines. According to the results, it can be stated that diametral point load test often gives lower values than those of axial test. This result can be attributed to the size effect of samples in point load test, as the L/D ratio increased more than 1.1 the $I_{s(a)}$ values increase more than $I_{s(d)}$. Moreover, axially loaded specimens with L/D ratio 1.1 give strength values equal to those of obtained in diametral testing (Broch and Franklin, 1972).

Block and cylindrical punch index

One of the practical strength index tests to indirectly determine the uniaxial compressive strength using disc-shaped specimens is the block punch index (BPI) test (Karakul *et al.*, 2010). In the current study, the test was conducted on the both mentioned directions. Besides, specimens with parallel lamination/bedding to the loading direction were punched by a loading plane (punching block) placed in normal direction to the lamination/bedding axis (Figs. 7 a and b). Thus, the lamination and bedding planes are taken into account by BPI test.

As shown in Table 2, the BPI values at the parallel direction for CDH, SKM, WAM and WDH specimens are 10.24, 9.82, 12.15 and 12.65 MPa

respectively. In comparison, the index values for the perpendicular direction of CDH, SKM, WAM and WDH specimens are 5.91, 7.71, 11.59 and 13.07 MPa respectively. It is evident from the results that BPI values of all travertine types (except WDH) are greater for the parallel direction to the lamination/bedding axis than perpendicular direction. Although, the WDH samples have lower n_ϕ and higher SSD values compared to other types, they indicate a relatively close laminated structure that usually makes it distinguished from the other types. Karakul *et al.*, (2010) reported similar results for a close banded travertine with BPI values approximately similar to those of WDH sample.

In this study, the cylindrical punch test (CPI) was applied to determine the cylindrical punch index (CPI) for travertine samples in two cutting directions. In comparison to BPI test, a limited number of research works have focused on the application of CPI test for anisotropic rocks. In all tested samples (except CDH), CPI values for parallel direction are lower than the values for perpendicular direction. In addition, the results of different travertine structures for both directions are similar to other tests, implying that CPI values follow the order of $CDH < SKM < WAM < WDH$. Interestingly, the CPI values are more similar to $I_{s(d)}$ results, since the rock samples were tested by applying a concentrated point load.

Uniaxial compressive strength

The σ_c of tested travertines varies from 48.82 to 85.13 MPa for parallel direction and 42.52 to 75.1 MPa for perpendicular direction. The minimum values of the parameter belong to CDH specimens

and maximum values to WDH specimens for both directions. Therefore, travertine strength parameters (σ_c , $I_{s(a)}$, $I_{s(d)}$, CPI, BPI, and σ_t) depend on the porosity of the rock, suggesting that the most porous rocks have the least strength values. In addition to porosity, the presence and percentage of sparite cement content especially with druzey mosaic and blocky textures affects the rock strength indirectly.

Some researchers reported that travertine strength especially σ_c has the highest values when the sample is loaded perpendicular to lamination/bedding axis irrespective to the structure and texture of the tested rocks (Karakul *et al.*, 2010; Ozcelik & Yilmazkaya, 2011; Yilmaz & Yucel, 2014). Çobanoğlu & Çelik (2012) reported the opposite situation that the strength values under parallel loading to lamination are higher than the perpendicular loading. According to these authors, calcite crystallization in porosities between laminations may raise the overall strength in parallel loading conditions. These results are consistent with those of Sengun *et al.*, (2015), who found the same results for travertines with pore degrees more than 9%. However, some other researchers indicated that mechanical behavior varies according to the predominant rock structure (García-del-Cura *et al.*, 2012).

They reported that the banded travertines with low-porous structure have the highest strength values when the rock is tested perpendicular to lamination/bedding axis. The explanation for this observation is that the discontinuity surfaces between bands, working as weakness planes when they are orientated parallel to the lamination/bedding axis.

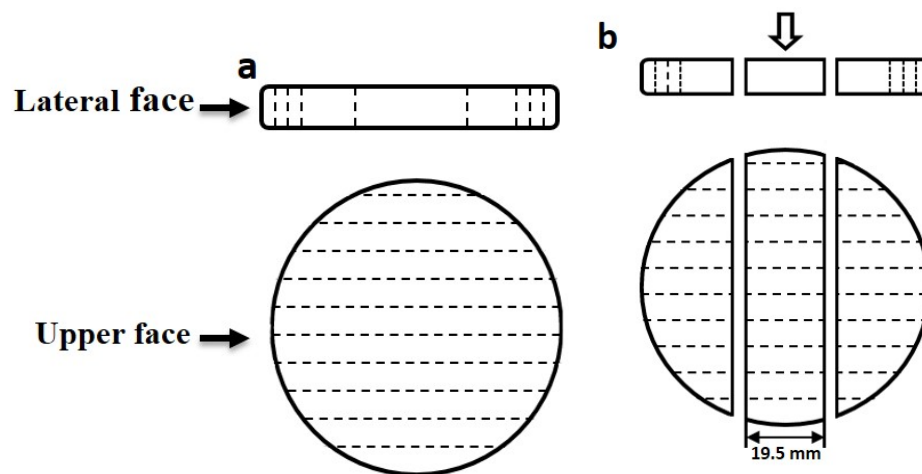


Figure 7. Schematic illustrations of the BPI test specimens with parallel lamination/bedding: (a) before and (b) after failure.

Therefore, the mechanical behavior of the studied travertines are not influenced by the rock structure, because the studied travertines are low-porous, except CDH which has both low-porous and porous samples. It can be seen from the results that rock porosity and to some extent sparite cement content should be considered as the most influential factors on mechanical behavior of these travertines. Nevertheless, the heterogeneity in lamination of WDH travertine caused a complexity in mechanical behavior of this type of travertine.

Generally, it is hard to decide which loading direction is more suitable for the construction and dimension stone industries, because it is different depending on the type of application, end product, visual appearance and the element which need to be built. For example, the highly porous travertine was used in parallel direction for columns in Khurheh temple, whereas for Atash-koh fire temple low porous travertine was utilized in perpendicular and parallel directions as rubble stones in the walls. In Atash-koh fire temple, walls with curved surfaces were built with the rubble stone in the parallel direction to the lamination/bedding axis and flat walls were built with the rubble stone in perpendicular conditions. Evidently, the travertines cut parallel to the lamination/bedding planes improve the outward appearance of walls or pillars.

Simple regression analysis for σ_c prediction

The relation between the σ_c and the geomechanical parameters for both cutting directions are plotted in Fig. 8. As seen in this figure, SSD has the best determination coefficient ($R = 0.75$ and 0.76) for predicting $\sigma_{c\perp}$ and $\sigma_{c\parallel}$ respectively. As noted by ASTM (2005) specification, this parameter only considers the specific gravity of permeable part of rocks which may be so effective for porous rocks like travertine.

Furthermore, σ_t shows very poor correlations ($R = 0.37$ and 0.42) with $\sigma_{c\perp}$ and $\sigma_{c\parallel}$, respectively. It should be noted that some physical and mechanical parameters such as n_ϕ , QAI, Vp and $I_{s(d)}$ indicate a higher correlation with $\sigma_{c\perp}$ and $\sigma_{c\parallel}$.

The relations between n_ϕ and σ_c for both directions were characterized by negative logarithmic functions. Such a trend was extracted between QAI and σ_c as well. The intersection of the fitting lines can be around 9.5% for n_ϕ and 3.5 % for QAI with the theoretical σ_c being around 35 MPa for both parameters. On the contrary, all other parameters (except Vp) show positive relations with

σ_c where most of the relations are characterized by linear equations. However, there are two exponential equations for $I_{s(a)}$ and σ_t versus $\sigma_{c\perp}$. All graphs follow two rules (except of Vp versus σ_c): 1) the intersection of the fitting lines is about 40 MPa, and 2) the slope of fitting lines for $\sigma_{c\parallel}$ is higher than fitting lines of $\sigma_{c\perp}$. Thus, it can be concluded that there is an overlapping between parallel and perpendicular results, and therefore the more porous travertines (CDH) have closer $\sigma_{c\perp}$ and $\sigma_{c\parallel}$ values. In addition, CDH, SKM and WAM samples, which have more similar structures and sparite content, show more overlapping between their results.

As mentioned earlier, Vp has an exceptional behavior especially for samples perpendicular to loading direction and shows lower $\sigma_{c\perp}$ values for low porous travertine (WDH) compared to WAM and SKM. Such a behavior can be related to the presence of close lamination in WDH samples which control the modulation of the ultrasonic waves through rocks. The presence of lamination in the perpendicular direction to the loading, leads to a decrease in wave propagation due to the gradually changing nature of the rock. Regarding such a behavior, Vp cannot be considered as a suitable parameter for quantifying rock anisotropy.

Multiple linear regression analysis for σ_c prediction

Multiple variable regression analysis was used to combine more than one parameter that affected the uniaxial compressive strength (σ_c) and to improve the accuracy of the obtained equations. The uniaxial compressive strength (perpendicular and parallel to the bedding/lamination axis; $\sigma_{c\perp}$ and $\sigma_{c\parallel}$) was correlated statistically with the 10 intact rock properties using multiple regression techniques. However, all mechanical parameters are similar and parallel strength parameters which their values are dependent to each other. Therefore, simple equations were previously proposed based on simple regression analyses, then an attempt has been made to combine only one strength and one physical parameter for developing more comprehensive models to predict σ_c .

For developing a multiple linear regression model, the training data set (2/3 of the total dataset) was firstly used and an equation was extracted, then input parameters of testing data set (1/3 of the total dataset) was fed into the equation to estimate σ_c and to validate the fitness of the prediction by training data set. In order to present the best suitable equations, models which are statistically significant at the 99% confidence level were chosen (Tables 5 and 7).

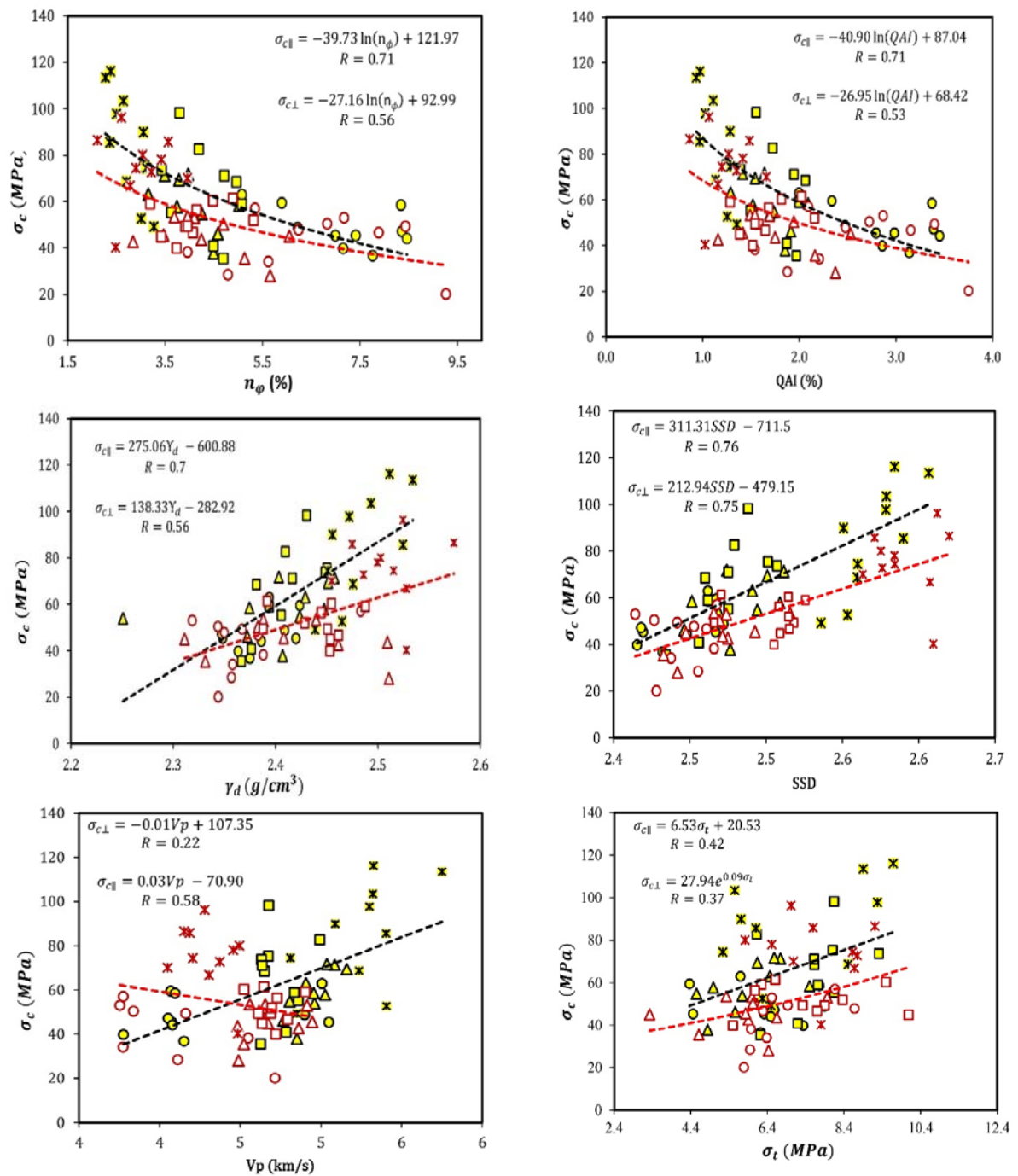


Figure 8. To be continued

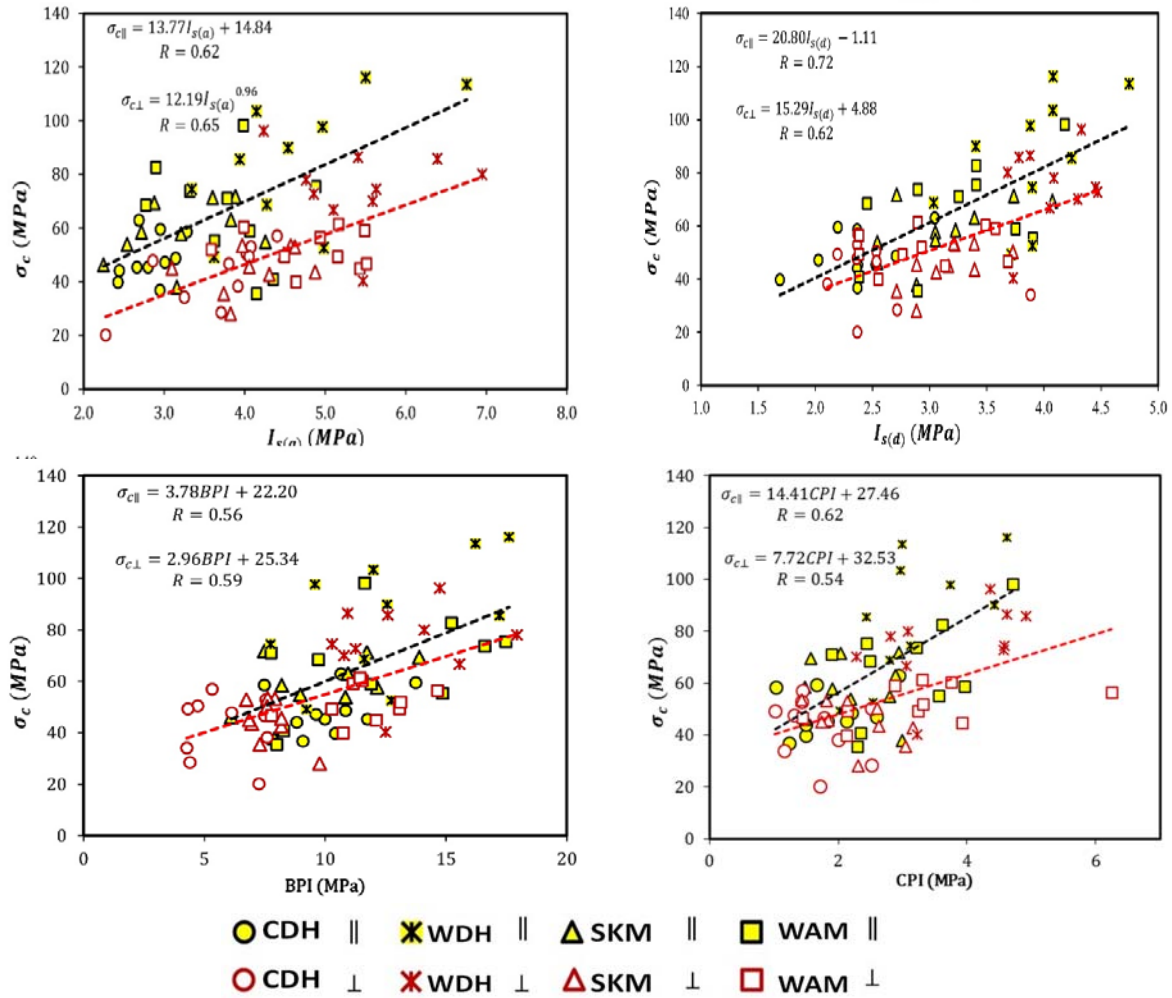


Figure 8. Relationship between the physico-mechanical properties and the uniaxial compressive strength of different travertine structures in case of parallel and perpendicular directions

For predicting $\sigma_{c||}$, all equations yield correlation coefficients $R > 0.75$ and p -value < 0.1 (Table 4 and 5). As mentioned, all equations are composed of two variables (one physical and one mechanical parameter). Of the engineering parameters, σ_c predicted from SSD associated with CPI, σ_t and $I_{s(a)}$ yield the best correlation statistics ($R > 0.82$, $RMSE < 12.97$, $ME < 0.36$ and $P < 0.1$; Eqs. 4-6). In addition, good correlations were found between γ_d and CPI variables and σ_c ($R = 0.88$, $RMSE = 12.25$, $ME = 0.54$ and $P < 0.1$; Eq. 3). Among these models, model 6 shows the highest R and lowest $RMSE$ and ME values. Both the training and testing results for model 6 are plotted in Fig. 9.

Although, determination coefficients of the models are not so strong, they are reliable and

accurate enough for travertines with heterogeneous fabric and porous structure.

As shown in Table 6 for $\sigma_{c\perp}$, model 1 based on the highest R and lowest $RMSE$ and ME values were considered as the best fits. This equation can be accepted as reliable estimates for $\sigma_{c\perp}$. Based on the t -test and T -test (Table 7), all the proposed models are statistically significant at the 99% confidence level. The relationship between the measured $\sigma_{c\perp}$ and values calculated from Eq. 1 in Fig. 10.

As expected from the previous models, SSD variable exists in some derived equations as this parameter has the strongest correlation with σ_c in simple regression ($R > 0.75$).

The other variable is CPI which is common in three of the proposed models for $\sigma_{c||}$ (models 3, 6, and 9).

Table 4. Statistic parameters (R, RMSE, ME) and equations for $\sigma_{c\parallel}$ models ($\sigma_{c\parallel}$: uniaxial compressive strength parallel to the lamination/bedding)

Model No.	Equations	Train			Test		
		R	RMSE (MPa)	ME (MPa)	R	RMSE (MPa)	ME (MPa)
1	$\sigma_{c\parallel} = -762 + 329.60 \gamma_d + 4.15 \sigma_t$	0.84	13.39	-0.48	0.79	16.06	3.13
2	$\sigma_{c\parallel} = -538 + 234.40 \gamma_d + 10.80 I_{s(a)}$	0.84	13.59	0.34	0.81	14.26	2.54
3	$\sigma_{c\parallel} = -630 + 276.10 \gamma_d + 9.54 CPI$	0.88	12.25	0.54	0.84	14.15	4.08
4	$\sigma_{c\parallel} = -673 + 281.60 SSD + 5.10 \sigma_t$	0.82	13.97	0.27	0.95	7.81	2.11
5	$\sigma_{c\parallel} = -383 + 162 SSD + 13.55 I_{s(a)}$	0.81	14.32	0.33	0.92	9.26	1.16
6	$\sigma_{c\parallel} = -531 + 227.60 SSD + 10.43 CPI$	0.86	12.97	0.36	0.92	9.54	1.27
7	$\sigma_{c\parallel} = -505 + 214.71 SSD + 3.11 BPI$	0.84	13.61	-0.09	0.80	12.82	-1.50
8	$\sigma_{c\parallel} = 55.20 - 7.70 n_\phi + 6.40 \sigma_t$	0.76	15.38	0.03	0.83	13.82	3.82
9	$\sigma_{c\parallel} = 55.10 - 4.40 n_\phi + 11.10 CPI$	0.75	15.65	-0.27	0.84	11.40	2.42
10	$\sigma_{c\parallel} = 45.10 - 5.05 n_\phi + 3.85 BPI$	0.79	14.75	0.00	0.69	16.07	1.21

Table 5. The statistical results of multiple regression analysis for $\sigma_{c\parallel}$

Model No.	Predictor	Coefficient	Standard error of coefficient	T	P-value	F	P-value
1	Constant	-762	145	-5.25	0.00	20.45	0.00
	γ_d	329.60	61.3	5.38	0.00		
	σ_t	4.15	2.14	1.94	0.00		
2	Constant	-538	215	-2.50	0.02	19.46	0.00
	γ_d	234.40	95.20	2.46	0.02		
	$I_{s(a)}$	10.80	6.34	1.71	0.10		
3	Constant	-630	144	-4.38	0.00	26.84	0.00
	γ_d	276.10	60.80	4.54	0.00		
	CPI	9.54	3.14	3.04	0.01		
4	Constant	-673	140	-4.82	0.00	17.80	0.00
	SSD	281.60	56.80	4.96	0.00		
	σ_t	55.10	2.19	2.32	0.00		
5	Constant	-383	214	-1.79	0.08	16.34	0.00
	SSD	162	92.30	1.76	0.09		
	$I_{s(a)}$	13.55	6.80	1.99	0.06		
6	Constant	-531	140	-3.80	0.00	22.59	0.00
	SSD	227.60	57.40	3.97	0.00		
	CPI	10.43	3.28	3.18	0.00		
7	Constant	-505	153	-3.29	0.00	19.58	0.00
	SSD	214.71	64.10	3.35	0.00		
	BPI	3.11	1.17	2.68	0.01		
8	Constant	55.20	19.3	2.86	0.01	12.59	0.00
	n	-7.70	1.93	-4.01	0.00		
	σ_t	6.40	2.38	2.68	0.01		
9	Constant	55.10	20.70	2.66	0.01	11.75	0.00
	n	-4.40	2.46	-1.81	0.08		
	CPI	11.10	4.49	2.47	0.02		
10	Constant	45.10	19.80	2.28	0.03	14.75	0.00
	n	-5.05	2.09	-2.41	0.02		
	BPI	3.85	1.22	3.15	0.00		

Table 6. Statistic parameters (R, RMSE, ME) and equations for $\sigma_{c\perp}$ models ($\sigma_{c\perp}$: uniaxial compressive strength perpendicular to the lamination/bedding)

Model No.	Equations	Train			Test		
		R	RMSE (MPa)	ME (MPa)	R	RMSE (MPa)	ME (MPa)
1	$\sigma_{c\perp} = -460.6 + 229.50 SSD - 0.01 Vp$	0.86	11.81	0.11	0.90	6.61	1.75
2	$\sigma_{c\perp} = -272 + 162.40 \gamma_d - 0.01 Vp$	0.74	14.75	0.52	0.68	9.79	-1.07
3	$\sigma_{c\perp} = -166 + 73.80 \gamma_d + 12.97 I_{s(a)}$	0.8	13.81	-0.58	0.7	9.29	2.75
4	$\sigma_{c\perp} = 172.10 - 6.79 n - 0.02 Vp$	0.73	14.92	1.11	0.69	9.48	2.56

Table 7. Summary of some parameters affecting the quality of model with six parameters. The statistical results of multiple regression analysis for $\sigma_{c\perp}$ models

Model No.	Predictor	Coefficient	Standard error of coefficient	T	P-value	F	P-value
1	Constant	-460.60	98.00	-4.7	0.00	19.86	0.00
	SSD	229.50	37.50	6.12	0.00		
	Vp	-0.01	0.01	-1.79	0.08		
2	Constant	-272	104	-2.61	0.02	8.45	0.00
	γ_d	162.40	41.30	3.93	0.00		
	Vp	-0.01	0.01	-1.66	0.10		
3	Constant	-166	112	-1.71	0.09	11.33	0.00
	γ_d	73.80	50	1.68	0.10		
	$I_{s(a)}$	12.97	5.12	2.53	0.02		
4	Constant	172.10	46	3.74	0.00	8.07	0.00
	n	-6.79	1.77	-3.84	0.00		
	Vp	-0.02	0.01	-2.02	0.05		

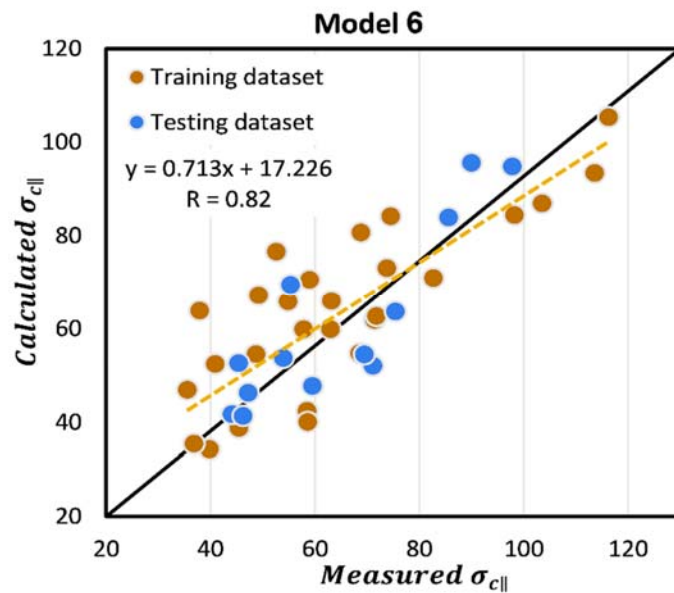


Figure 9. The relationship between measured and calculated values for $\sigma_{c\parallel}$

Surprisingly, σ_t parameter is presented in other three models proposed for predicting $\sigma_{c\parallel}$ and, despite its very low correlation with σ_c in simple regression

($R < 0.42$). Therefore, the proposed equations are not necessarily composed of parameters with the higher/stronger correlation coefficient in simple

regression. The derived equations in this study were compared with those available in the literature (Table 8).

It is worth to noting that there is a significant difference between the results of this study and other researches. Firstly, only a few researchers considered more than one parameter to evaluate σ_c of travertines; secondly, a few literatures only

mentioned to cutting direction and predicting σ_c of travertines in both cutting directions.

Although, most of the literatures mentioned that there is correlation coefficients (R) less than 0.9 exist between σ_c and geomechanical parameters especially Akin and Özsan, (2011) who presented a low correlation coefficient between n and σ_c ($\sigma_{c\parallel}$: R = 0.67).

Table 8 Derived regression equations and correlation coefficients (R) proposed by different researchers

Rock type	Rock parameters	Equations	Reference	R
Travertine	n	$\sigma_{c\parallel} = 47.76 n^{-0.31}$	Akin & Özsan (2011)	0.67
		$\sigma_{c\perp} = 92.10 n^{-0.74}$		0.88
Travertine	Vp n Rn	$\sigma_c = -595.3 - 442.4 Vp + 45.3 Vp^2 - 6.1n + 0.5 n^2 + 28.3 Is - 4.1 Is^2 + 115.8 Rn - 2 Rn^2$	Dehghan <i>et al.</i> (2010)	0.8
Travertine	γ_d	$\sigma_c = 0.06 e^{2.92\gamma_d}$	Çobanoğlu & Çelik (2010)	0.84
Limestone, sandstone, mica schist, shale and travertine	BPI	$\sigma_{c\perp} = 5.1 \times 1.47^{-0.00456\alpha} BPI_{\perp}$	Karakul <i>et al.</i> (2010)	-
Travertine	n Vp	$\sigma_{c\perp} = 204.37 n_{\phi}^{-0.70}$	Török & Vásárhelyi (2010)	0.87
		$\sigma_{c\perp} = 0.547 Vp^{3.11}$		0.9
Travertine	Vp	$\sigma_{c\perp} = 101.10 Vp - 802.80$	Jamshidi <i>et al.</i> (2016)	0.97

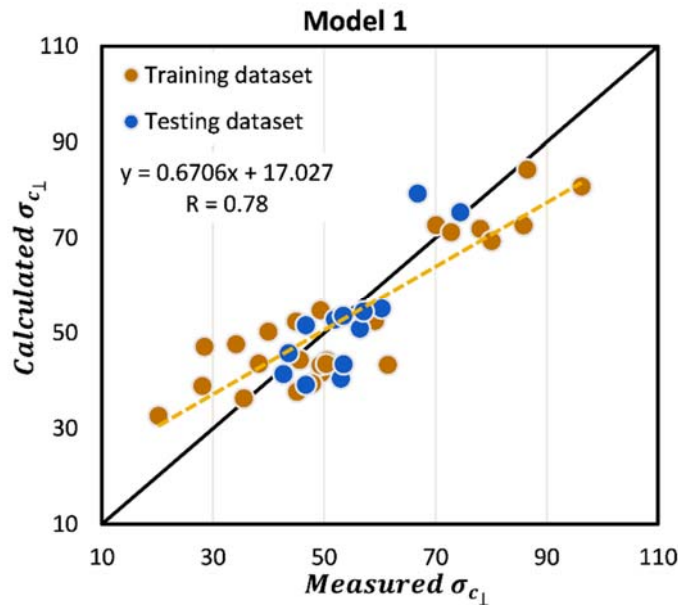


Figure 10. The relationship between measured and calculated values for $\sigma_{c\perp}$

This shows, it is so common to exist such a low correlation coefficient between σ_c and other parameters.

Conclusions

The present work is conducted to assess σ_c of travertines using simple index tests considering the orientations of the lamination axis. These travertine specimens were chosen as a representative for both modern and historical building stones in the study area. It should be noted that the results of this research only can be used for the studied travertines and each type of travertine may demonstrate different behavior.

Among geomechanical parameters, SSD has the most notable effect on predicting σ_c . The order of geomechanical properties of the studied travertines were revealed as WDH > WAM > SKM > CDH. Due to the presence of higher amount of microcrystalline mud (micrite) matrix which had loose packing and low strength, it was expected that WAM has lower strength parameters than SKM and CDH; therefore, porosity is more important than micrite content. According to the obtained results, the effect of porosity is more than matrix type and these are more influential than rock structure and texture on rock strength. Unlike our expectation that the increase in sparite content, i.e. the increase in size of grain and crystals, led to decrease in the strength parameters, it was found that the sparite cement joins the mud grains (micrite which is so loose) and increased the rock strength. Accordingly, WDH sample has the highest strength parameters in comparison to other types of travertines.

The cutting direction has a crucial impact on structure, texture, type and percentage of matrix and pore degree. The results mainly indicate that most of the mechanical parameters have greater values when

stress is applied in parallel to the longest direction of the pores than perpendicular direction. Although, travertine is an anisotropic rock, wide bands and irregular laminations did not make weakness planes to reduce rock strength for parallel loading direction. On the other hand, when the travertines are loaded parallel to the longest direction of pores, the stress is applied in an x-y plane not in the z-direction (the longest direction of pores); as a result, the strength of travertines increases in the z-direction. Thus, the most notable factors affecting the strength of anisotropic travertine are geometry, intensity, and the longest direction of pores. The results of statistical analyses revealed that SSD, σ_t and CPI are the best parameters to determine $\sigma_{c\parallel}$ and also some parameters such as SSD and Vp increase R value especially for the $\sigma_{c\perp}$.

On the other hand, the poor correlation coefficients obtained for all parameters relate to the highly heterogeneous texture and structure of the studied travertines. Also, these correlation coefficients show that simple and multiple regression are not suitable analyses to find parameters which are more related to σ_c , which means some soft computing methods should be used to find the better correlation of σ_c with geomechanical parameters.

Acknowledgement

This study was financed by the University of Bu-Ali Sina, department of geology.

Our special thanks are offered to Mr H.R. Mirzaiee (the chief of Sajad stone factory) who is provided and cut the studied travertine blocks in desirable sizes. We would like to thank Dr H. Mohsseni (Associated professor in sedimentary geology) and Dr S. Rahmani (PhD in sedimentary geology) for their valuable suggestions on petrography of the studied rocks.

References

- Akin, M., Özsan, A., 2011. Evaluation of the long term durability of yellow travertine using accelerated weathering tests. *Bulletin of engineering geology and the environment*, 70: 101-114.
- Akyol, E., Yagiz, S., Ozkul, M., Sen, G., Kato, S., 2005. Physical properties of hot spring travertines related to lithotypes at Pamukkale region in Denizli, Turkey. In: *Int. Symposium on Travertine*, September 21-25, Denizli Turkey, pp 286-290.
- ASTM, D-6473-15 (Reapproved 2005), Standard test method for specific gravity and absorption of rock for erosion control ASTM standards on disc 0409 designation.
- ASTM, D-4543-85 (Reapproved 1991), Standard practice for preparing rock core specimens and determining dimensional and shape tolerances. *Annual book of ASTM standards*, Section 4.
- Broch, E., Franklin, J., 1972. The point-load strength test. In: *International Journal of Rock Mechanics and Mining Sciences & Geomechanics Abstracts*, 6: 669-676.
- Brown, E., 1981a. ISRM suggested methods. Rock characterization testing and monitoring. Pergamon Press, Oxford.
- Brown, E., 1981b. Suggested methods for determining the uniaxial compressive strength and deformability of rock materials Rock characterization, testing and monitoring-*ISRM suggested methods* Pergamon Press, Oxford:113-116

- Cargill, J. S., 1990. Shakoor A Evaluation of empirical methods for measuring the uniaxial compressive strength of rock. In: *International Journal of Rock Mechanics and Mining Sciences & Geomechanics Abstracts*, 6: 495-503.
- Chentout, M., Alloul, B., Rezouk, A., Belhai, D., 2015. Experimental study to evaluate the effect of travertine structure on the physical and mechanical properties of the material. *Arabian Journal of Geosciences* 8: 8975-8985.
- Çobanoğlu, İ., Çelik, S. B., 2012. Determination of strength parameters and quality assessment of Denizli travertines (SW Turkey). *Engineering Geology*, 129: 38-47.
- D'Andrea, D. V., Fischer, R., Fogelson, D., 1965. Prediction of compressive strength from other rock properties vol 6702. US Dept. of the Interior, Bureau of Mines.
- Dehghan, S., Sattari, G., Chelgani, S. C., Aliabadi, M., 2010. Prediction of uniaxial compressive strength and modulus of elasticity for Travertine samples using regression and artificial neural networks. *Mining Science and Technology (China)*, 20: 41-46.
- Erdoğan, O., Özvan, A., 2015. Evaluation of strength parameters and quality assessment of different lithotype levels of Edremit (Van) Travertine (Eastern Turkey). *Journal of African Earth Sciences*, 106: 108-117.
- Ersoy, A., Atıcı, U., Büyüksağış, I., 2005. The assessment of the specific cutting energy in travertine. In: *Proceedings of 1st International Symposium on Travertine*, Pamukkale University, 217-223.
- Franklin, J., 1985. Suggested method for determining point load strength. In: *International Journal of Rock Mechanics and Mining Sciences & Geomechanics Abstracts*, 2: 51-60.
- Folk, R.L., 1962. Spectral subdivision of limestone types.
- García-del-Cura, M. Á., Benavente, D., Martínez-Martínez, J., Cueto, N., 2012. Sedimentary structures and physical properties of travertine and carbonate tufa building stone. *Construction and Building Materials*, 28:456-467
- Ghorbani Dashtaki, S., Homaei, M., Mahdian, M.H., Kouchakzadeh, M., 2009. Site-dependence performance of infiltration models. *Water resources management*, 23: 2777-2790.
- Gokce, M. V., 2015. The effects of bedding directions on abrasion resistance in travertine rocks. *Turkish Journal of Earth Sciences*, 24: 196.
- Gokceoglu, C., 2002. A fuzzy triangular chart to predict the uniaxial compressive strength of the Ankara agglomerates from their petrographic composition. *Engineering Geology*, 66: 39-51.
- Irfan, T., 1996. Mineralogy, fabric properties and classification of weathered granites in Hong Kong. *Quarterly Journal of Engineering Geology and Hydrogeology*, 29: 5-35.
- ISRM, 1978. Suggested methods for determining tensile strength of rock materials. In: *International Journal of Rock Mechanics and Mining Sciences & Geomechanics Abstracts*, 15.
- Jamshidi, A., Nikudel, M.R., Khamechiyan, M., Sahamieh, R.Z., Abdi, Y., 2016. A correlation between P-wave velocity and Schmidt hardness with mechanical properties of travertine building stones. *Arabian Journal of Geosciences*, 9:568
- Karakul, H., Ulusay, R., Isik, N., 2010 Empirical models and numerical analysis for assessing strength anisotropy based on block punch index and uniaxial compression tests. *International Journal of Rock Mechanics and Mining Sciences*, 47: 657-665.
- Khanlari, G.R., Heidari, M., Sepahigero, A.A., Fereidooni, D., 2014. Quantification of strength anisotropy of metamorphic rocks of the Hamedan province, Iran, as determined from cylindrical punch, point load and Brazilian tests. *Engineering Geology*, 169: 80-90
- Khanlari, G., Heidari, M., Momeni, A., Abdilor, Y., 2012. Prediction of shear strength parameters of soils using artificial neural networks and multivariate regression methods. *Engineering Geology*, 131: 11-18.
- Kohno, M., Maeda, H., 2012. Relationship between point load strength index and uniaxial compressive strength of hydrothermally altered soft rocks. *International Journal of Rock Mechanics and Mining Sciences*, 50: 147-157.
- Koncagül, E.C., Santi, P.M., 1999. Predicting the unconfined compressive strength of the Breathitt shale using slake durability, Shore hardness and rock structural properties. *International Journal of Rock Mechanics and Mining Sciences*, 36: 139-153.
- Legates, D.R., McCabe, G.J., 1999 Evaluating the use of “goodness of fit” measures in hydrologic and hydroclimatic model validation. *Water Resources Research*, 35: 233-241.
- Mishra, D., Basu, A., 2012 Use of the block punch test to predict the compressive and tensile strengths of rocks. *International Journal of Rock Mechanics and Mining Sciences*, 51: 119-127.
- Montgomery, D.C., Peck, E.A., Vining, G.G., 2015. *Introduction to linear regression analysis*. John Wiley & Sons.
- Ozcelik, Y., Polat, E., Bayram, F., Ay, A., 2004. Investigation of the effects of textural properties on marble cutting with diamond wire. *International Journal of Rock Mechanics and Mining Sciences*, 41: 228-234.
- Ozcelik, Y., Yilmazkaya, E., 2011. The effect of the rock anisotropy on the efficiency of diamond wire cutting machines. *International Journal of Rock Mechanics and Mining Sciences*, 48: 626-636.
- Pentecost, A., 2005 *Travertine*. Springer Science & Business Media.
- Rilem, T-25-PEM, 1980. Recommended tests to measure the determination of stone and to assess the effectiveness of treatment methods materials and structures. 13: 175-253
- Saroglou, H., Marinos, P., Tsiambaos, G., 2004. The anisotropic nature of selected metamorphic rocks from Greece. *Journal*

- of the South African Institute of Mining and Metallurgy 104: 217-222.
- Sengun, N., Demirdag, S., Ugur, I., Akbay, D., Altindag, R., 2015. Assessment of the physical and mechanical variations of some travertines depend on the bedding plane orientation under physical weathering conditions. *Construction and Building Materials*, 98: 641-648.
- Shakoor, A., Bonelli, R.E. 1991. Relationship between petrographic characteristics, engineering index properties, and mechanical properties of selected sandstones. *Environmental & Engineering Geoscience*, 28:55-71.
- Shalabi, F.I., Cording, E.J., Al-Hattamleh, O.H., 2007. Estimation of rock engineering properties using hardness tests. *Engineering Geology*, 90: 138-147.
- Sharma, P., Khandelwal, M., Singh, T., 2011. A correlation between Schmidt hammer rebound numbers with impact strength index, slake durability index and P-wave velocity. *International Journal of Earth Sciences*, 100: 189-195.
- Sharma, P., Singh, T., 2008. A correlation between P-wave velocity, impact strength index, slake durability index and uniaxial compressive strength. *Bulletin of Engineering Geology and the Environment*, 67: 17-22.
- Singh, V., Singh, D., Singh, T., 2001. Prediction of strength properties of some schistose rocks from petrographic properties using artificial neural networks. *International Journal of Rock Mechanics and Mining Sciences*, 38:269-284.
- Sulukcu, S., Ulusay, R., 2001. Evaluation of the block punch index test with particular reference to the size effect, failure mechanism and its effectiveness in predicting rock strength. *International Journal of Rock Mechanics and Mining Sciences*, 38: 1091-1111.
- Suwansawat, S., Einstein, H.H., 2006. Artificial neural networks for predicting the maximum surface settlement caused by EPB shield tunneling. *Tunnelling and Underground Space Technology*, 21: 133-150.
- Torabi-Kaveh, M., Naseri, F., Saneie, S., Sarshari, B., 2015. Application of artificial neural networks and multivariate statistics to predict UCS and E using physical properties of Asmari limestones. *Arabian Journal of Geosciences*, 8: 2889-2897.
- Török, Á., Vásárhelyi, B., 2010. The influence of fabric and water content on selected rock mechanical parameters of travertine, examples from Hungary. *Engineering Geology*, 115: 237-245.
- Ulusay, R., Türeli, K., Ider, M., 1994. Prediction of engineering properties of a selected litharenite sandstone from its petrographic characteristics using correlation and multivariate statistical techniques. *Engineering Geology*, 38: 135-157.
- Ulusay, R., Gokceoglu, C., Sulukcu, S., 2001. Draft ISRM suggested method for determining block punch strength index (BPI). *International Journal of Rock Mechanics and Mining Sciences*, 38: 1113-1119.
- Vernik, L., Bruno, M., Bovberg, C., 1993. Empirical relations between compressive strength and porosity of siliciclastic rocks. In: *International Journal of Rock Mechanics and Mining Sciences & Geomechanics Abstracts*, 7: 677-680.
- Yagiz, S., 2009. Predicting uniaxial compressive strength, modulus of elasticity and index properties of rocks using the Schmidt hammer. *Bulletin of Engineering Geology and the Environment*, 68: 55-63.
- Yagiz, S., 2012. Comments on “Determination of strength parameters and quality assessment of Denizli travertines (SW Turkey)” Ibrahim Cobanoglu and Sefer Beran Celik, 129–130 (2012) 38–47. *Engineering Geology*, 147: 149-150.
- Yesiloglu-Gultekin, N., Sezer, E.A., Gokceoglu, C., Bayhan, H., 2013. An application of adaptive neuro fuzzy inference system for estimating the uniaxial compressive strength of certain granitic rocks from their mineral contents. *Expert Systems with Applications*, 40: 921-928.
- Yilmaz, I., Yucel, Ö., 2014. Use of the core strangle test for determining strength anisotropy of rocks. *International Journal of Rock Mechanics and Mining Sciences*, 66: 57-63.
- Zarif, I., Tuğrul, A., 2003. Aggregate properties of Devonian limestones for use in concrete in Istanbul, Turkey. *Bulletin of Engineering Geology and the Environment*, 62: 379-388.